Journal of Colloid and Interface Science 362 (2011) 261–266

Contents lists available at ScienceDirect

Journal of Colloid and Interface Science

www.elsevier.com/locate/jcis

Tailoring the carbon nanostructures grown on the surface of Ni–Al bimetallic nanoparticles in the gas phase

Whi Dong Kim [a], Ji Young Ahn [a], Dong Geun Lee [b], Hyung Woo Lee [c], Suck Won Hong [d], Hyun Seol Park [e], Soo H. Kim [a,*]

[a] Department of Nanosystem and Nanoprocess Engineering, College of Nanoscience and Nanotechnology, Pusan National University, 30 Jangjeon-dong, Geumjung-gu, Busan 609-735, Republic of Korea
[b] School of Mechanical Engineering, Pusan National University, 30 Jangjeon-dong, Geumjung-gu, Busan 609-735, Republic of Korea
[c] National Core Research Center for Hybrid Materials Solution, Pusan National University, 30 Jangjeon-dong, Geumjung-gu, Busan 609-735, Republic of Korea
[d] Department of Nanomaterials Engineering, College of Nanoscience and Nanotechnology, Pusan National University, 30 Jangjeon-dong, Geumjung-gu, Busan 609-735, Republic of Korea
[e] Clean Energy System Research Center, Korea Institute of Energy Research, Yuseong-gu, Daejeon 305-343, Republic of Korea

ARTICLE INFO

Article history:
Received 4 January 2011
Accepted 16 June 2011
Available online 25 June 2011

Keywords:
Carbon nanostructures
Bimetallic nanoparticles
Spray pyrolysis
Thermal chemical vapor deposition
Aerosol synthesis

ABSTRACT

A gas-phase, one-step method for producing various aerosol carbon nanostructures is described. The carbon nanostructures can be selectively tailored with either straight, coiled, or sea urchin-like structures by controlling the size of Ni–Al bimetallic nanoparticles and the reaction temperature. The carbon nanostructures were grown using both conventional spray pyrolysis and thermal chemical vapor deposition. Bimetallic nanoparticles with catalytic Ni (guest) and non-catalytic Al (host) matrix were reacted with acetylene and hydrogen gases. At the processing temperature range of 650–800 °C, high concentration straight carbon nanotubes (S-CNTs) with a small amount of coiled carbon nanotubes (C-CNTs) can be grown on the surface of seeded bimetallic nanoparticle size <100 nm, resulting from consumption of the melting Al matrix sites; sea urchin-like carbon nanotubes (SU-CNTs) of small diameter (~10 ± 4 nm) can be grown on the bimetallic nanoparticle size >100 nm, resulting from the significant size reduction of the available Ni sites due to thermal expansion of molten Al matrix sites without consumption of Al matrix. However, at the processing temperature range of 500–650 °C, C-CNTs can be grown on the bimetallic nanoparticle size <100 nm due to the presence of Al matrix in the bimetallic nanoparticles; SU-CNTs of large diameter (~60 ± 13 nm) can also be grown on the bimetallic nanoparticle size >100 nm due to the isolation of Ni sites in the Al matrix.

1. Introduction

The diameter and length of straight carbon nanotubes (CNTs) greatly influence CNT mechanical, chemical, and electrical properties [1,2]. Additionally, altering the shapes of CNT nanostructures modifies or adjusts multiple CNT functions. For instance, CNTs in the shape of coils or helixes are used as potential building blocks for electromagnetic shields [3], nano springs [4], and microsensor systems [5]. Researchers have attempted various gas-phase synthetic fabrication methods for forming aerosol CNTs. These endeavors resulted from the advantages of simple, easy, inexpensive and continuous production of high purity CNTs in the gas phase [6]. Unlike substrate-grown CNTs, however, the controllability of dimension and shape of CNTs in the gas phase is relatively difficult to achieve because the size and shape of seeded catalytic particles continuously change due to the competition between coagulation and coalescence processes prior to or during the chemical vapor deposition (CVD)-assisted growth of CNTs accompanied by relatively high temperature processes.

The various CNT nanostructures were formed on the catalytic particles dispersed on a given substrate under a sufficient reaction time of longer than several minutes in a vacuum [7–9]. However, few reports exist on the gas-phase formation of aerosol CNTs with various nanostructures under a relatively short reaction time of less than 1 min and atmospheric pressure conditions [10–14]. Recently, we unexpectedly observed that the mixtures of straight, coiled, and sea urchin-like aerosol CNTs formed over the entire surface of floating bimetallic nanoparticles of which the initial chemical composition Ni:Al was equal to a 1:1 M ratio and a reaction time of approximately 1 min, as shown in Fig. 1a. Here, straight CNT (S-CNT, Fig. 1b) is a single straight CNT, coiled CNT (C-CNT, Fig. 1c) is a single coiled CNT, and sea urchin-like CNT (SU-CNT, Fig. 1d) is multiple straight CNTs grown in a given Ni–Al bimetallic nanoparticle. The Ni was used as catalytic guest sites for nucleating, and

* Corresponding author.
E-mail address: sookim@pusan.ac.kr (S.H. Kim).

0021-9797/$ - see front matter © 2011 Elsevier Inc. All rights reserved.
doi:10.1016/j.jcis.2011.06.043

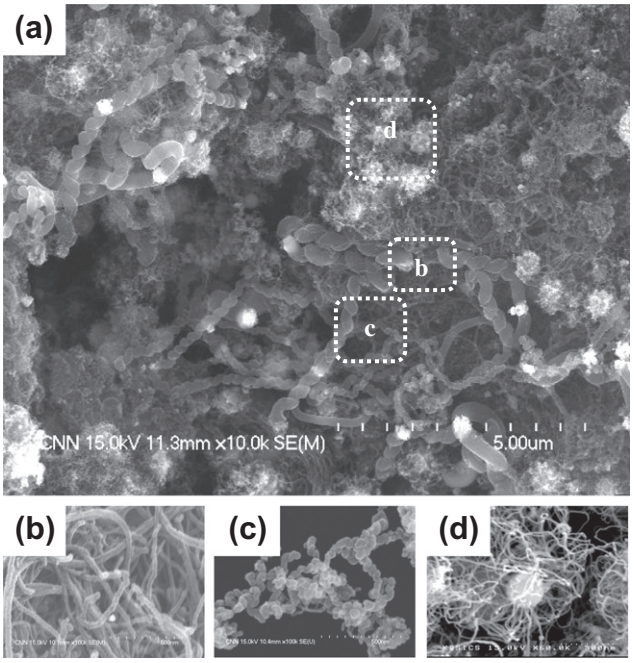

Fig. 1. (a) SEM image of the aerosol CNTs with various nanostructures (i.e. (b) straight CNTs(S-CNTs), (c) coiled CNTs(C-CNTs), (d) sea urchin-like CNTs (SU-CNTs)) directly grown on spray pyrolized bimetallic particles via. thermal CVD process at 800 °C.

subsequently growing CNTs; whereas, the Al was used as non-catalytic host matrix sites for homogeneously dispersing the Ni sites. At this point, we investigated the formation of morphological variations in the resulting aerosol CNTs. Fig. 1 displays the scanning electron microscope (SEM) image of various CNTs. After closer inspection of Fig. 1, we can conclude that the size of seeded bimetallic particles and the reacting temperature for growing CNTs must be key factors in determining the final CNT nanostructures. Therefore, possible growth mechanisms of various aerosol carbon nanostructures which formed on the bimetallic nanoparticles suspended in the gas phase were studied, followed by proposals for possible strategies that tune the shapes of aerosol CNTs with straight, coiled and sea urchin-like nanostructures.

2. Experimental

A single-step conventional spray pyrolysis combined with a subsequent thermal CVD was employed in order to grow aerosol CNTs on the floating catalysts [15]. Aluminum nitrate nonahydrate ($Al(NO_3)_3{\cdot}9H_2O$, Sigma Aldrich) and nickel nitrate hexahydrate ($Ni(NO_3)_3{\cdot}6H_2O$, Sigma Aldrich) at a 1:1 M ratio were dissolved in deionized water with a total concentration of 3 wt.%. The metal nitrate aqueous solution was aerosolized into micron-sized droplets using a homemade ultrasonic nebulizer operated at 40 W and 60 Hz, and then they were carried with a controlled nitrogen gas flow of approximately 1 lpm. After passing through a silica-gel dryer, the evaporating aerosol droplets contained bimetallic nitrates were rapidly solidified. Subsequently, the droplets transformed into pure bimetallic nanoparticles by thermal decomposition and hydrogen reduction (H_2 = ~100 sccm) processes in the first quartz reactor (2.54 cm diameter × 30 cm heating length) enclosed by an electric furnace heated at ~1000 °C. Here, the geometric mean diameter (GMD) of the bimetallic nanoparticles was found to be ~300 nm, which were in situ measured by using a scanning mobility particle sizer (SMPS, HCT, Inc., Model No. 4312). The pure bimetallic nanoparticles formed were then rapidly transported into the second quartz reactor (5.08 cm diameter × 30 cm heating length) enclosed by an electric furnace (thermal CVD reactor) heated at various temperature ranges of 500–800 °C, in which they were simultaneously reacted with controlled amount of acetylene (C_2H_2 = ~10 sccm) and hydrogen (H_2 = ~100 sccm) gases to grow aerosol CNTs with the residence time of ~50 s. The resulting aerosol CNTs were finally collected on the membrane filter with pore size of ~200 nm.

3. Results and discussion

A closer look at Fig. 1 reveals that the relatively small sized bimetallic particles are favorable for growing both straight CNTs (S-CNTs) and coiled CNTs (C-CNTs). Alternatively, the relatively large sized bimetallic particles seemed to be conducive for growing multiple CNTs that resembled 'sea urchin' (SU-CNTs). In order to first identify the role of size of bimetallic particles, the bimetallic aerosol nanoparticles with three different average sizes (D_p) of 60 ± 10 nm (Fig. 2a), 200 ± 60 nm (Fig. 2b), and 300 ± 95 nm (Fig. 2c), respectively, were selected by using a differential mobility analyzer (DMA, HCT, Inc., Model No. 4210). The DMA is an electrostatic classifier composed of a negatively charged high voltage-connected inner cylindrical electrode and electrical ground-connected outer cylindrical electrode. When polydisperse particles are introduced with sheath gas (N_2 = ~10 lpm), the particles experience the force balance between an electrostatic attraction force and a drag force so that a group of monodisperse particles with the same electrical mobility at a certain applied voltage pass through the slit located on the bottom of DMA [16,17]. The bimetallic aerosol nanoparticles with relatively uniform diameter selected by the DMA were then mixed with hydrogen and pyrolyzed at 1000 °C in the spray pyrolysis reactor, and subsequently introduced into the thermal CVD reactor mixed with acetylene and hydrogen for directly growing CNTs at 800 °C. It was observed that the mixtures of S-CNTs and C-CNTs were grown on the surface of bimetallic nanoparticles with the average size of smaller than ~100 nm (see Fig. 2d), while SU-CNTs were mostly grown on the surface of bimetallic nanoparticles with the average size of larger than ~100 nm as shown in Fig. 2e and f.

The possible reason for the formation of S-CNT or C-CNT is attributed to the significant reduction in the size of seeded bimetallic particles (i.e., D_p < ~100 nm), which decreased the sizes of both Ni and Al sites in the bimetallic particles so that the role of Al as a host matrix for isolating Ni sites was significantly deteriorated. Simultaneously, the catalytic Ni sites were densely located and even connected, to some extent, as a single Ni cluster.

Therefore, when the small sized bimetallic nanoparticle (i.e., D_p < ~100 nm) reacted with incoming hydrocarbon gas in the thermal CVD reactor, a single CNT tends to be catalytically formed on the entire surface of the seeded bimetallic nanoparticle. Unlike the growth of S-CNT and C-CNT, SU-CNTs are grown on every available Ni site, which are sufficiently isolated by the presence of Al host matrix sites in the sufficiently large bimetallic particles (i.e., D_p > ~100 nm).

The different growth patterns of the S-CNT and C-CNT, which both possessed the same initial chemical composition and were both grown on small sized bimetallic nanoparticles (i.e., D_p < ~100 nm), required further investigation. The observation generally follows that the S-CNTs were grown on pure Ni nanoparticles, while C-CNTs initially formed on the Ni nanoparticles mixed with an Al component. Several studies have previously suggested that the extreme difference in the wettability of bimetallic components to graphite (e.g., contact angles of Ni and Al to graphite are <75° and 159°, respectively) trigger the coupled attraction and repulsive forces, which promote the anisotropic growth of CNT on the surface of bimetallic nanoparticles seeded [18,19]. The mismatches in the

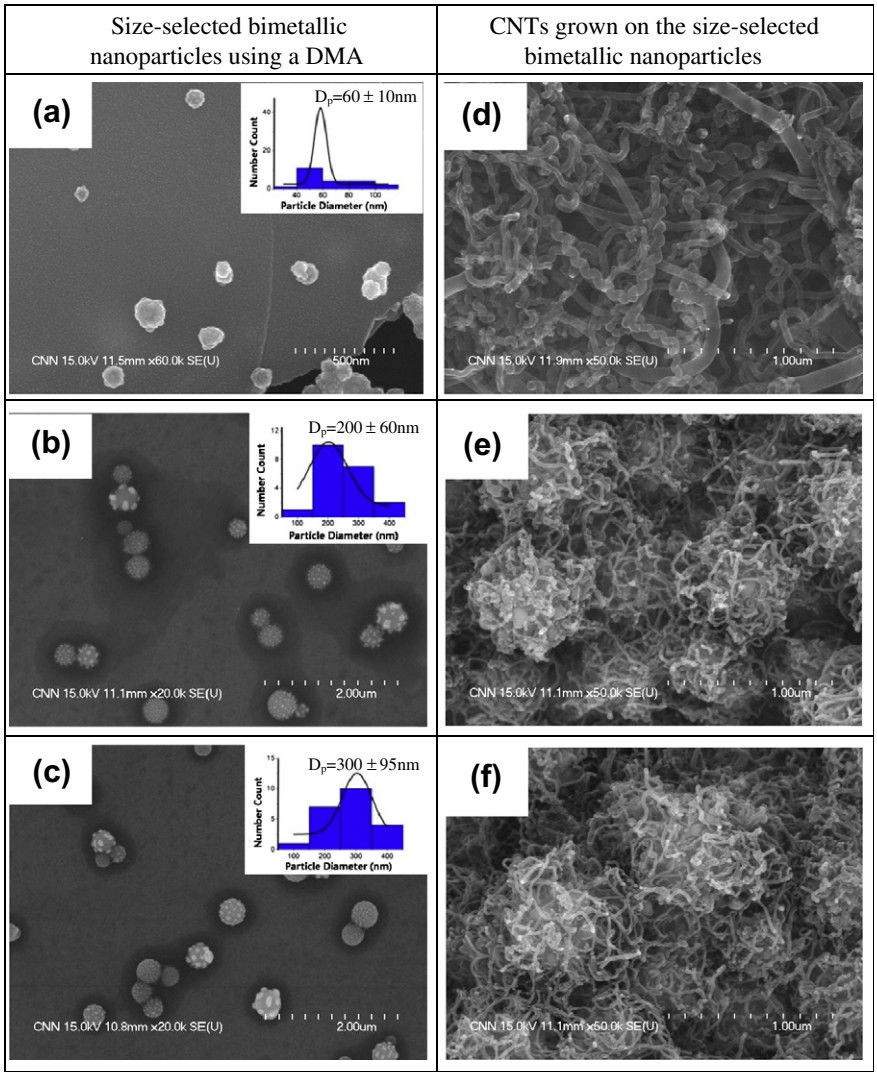

Fig. 2. SEM images of monodisperse bimetallic nanoparticles with the average size of (a) 60 ± 10 nm, (b) 200 ± 60 nm, and (c) 300 ± 95 nm selected by a DMA (the inserts are the number count of particles as a function of particle diameter), and the resulting CNTs grown accordingly on the size-selected bimetallic nanoparticles at 800 °C with the nanostructures of (d) the mixture of S-CNTs and C-CNTs and (e and f) SU-CNTs.

growth rate of CNT on the basal plane of the bimetallic particle impose stress–strain on the graphite layer precipitated so that the extrusion of CNT was bent or kinked. The possible formation of pentagonal or heptagonal meshes in the graphite network (i.e., hexagonal structure) was made at the molecular level, which relieved long-term stress–strain conditions [20]. However, this simplified hypothesis does not sufficiently account for the regular formation of constant pitch in the C-CNTs. The presence of Al component in the Ni nanoparticles is very important to determine the formation of C-CNTs.

Raman spectra for C-CNTs and SU-CNTs as shown in Fig. 3 corroborate the formation of multi-walled CNTs by showing strong peaks at ~1350 cm^{-1} (D mode, disorder-induced band originating from defects or carbon impurities) and ~1600 cm^{-1} (G mode, stretching mode in the graphite plane) without significant spectra at the low frequency in the radial breathing mode. Furthermore, the full width at half-maximum (FWHM)-based D/G ratio at ~1350 and ~1600 cm^{-1} (i.e., I_{1350}/I_{1600}, where I is intensity) is found to be ~1.5 for C-CNTs and ~0.9 for SU-CNTs, respectively, suggesting that C-CNTs had considerable disorders which were presumably induced by the presence of pentagon–heptagon pairs in the graphite nanostructures, while SU-CNTs had a relatively high degree of graphitization.

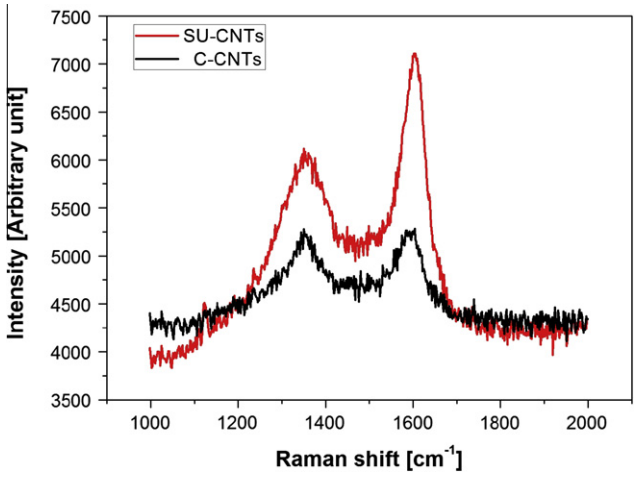

Fig. 3. Raman spectra of aerosol C-CNTs and SU-CNTs grown on the bimetallic particles at 800 °C.

In order to adjust the shape of CNTs from straight to coiled structures, the Al component must be maintained in the Ni nano-

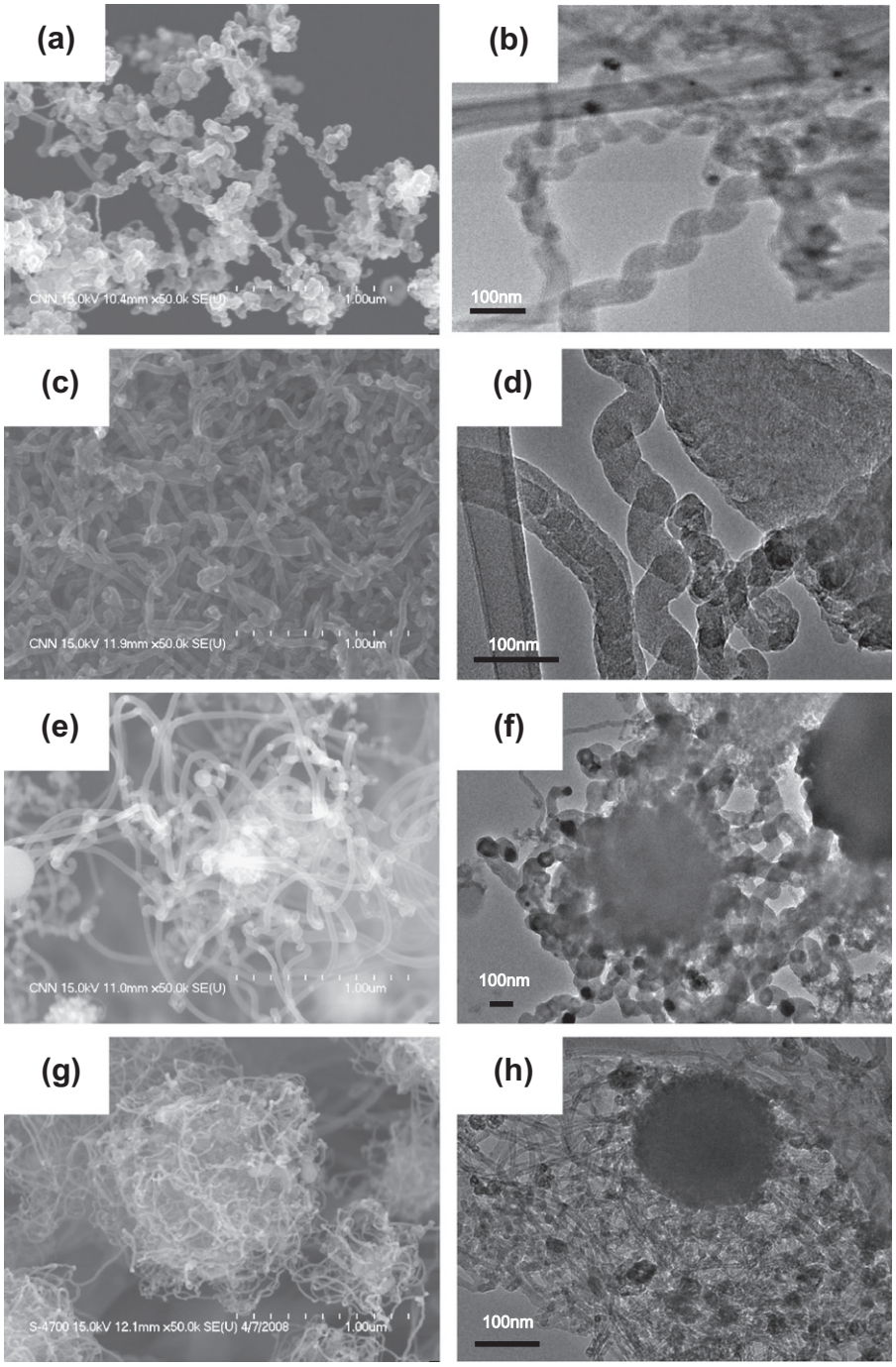

Fig. 4. SEM and TEM images of CNTs grown under the various experimental conditions of (a and b) D_p = ~50 nm, T_G = 500 °C [C-CNTs formed with D_{CNT} = ~50 ± 10 nm], (c and d) D_p = ~50 nm, T_G = 700 °C [S-CNTs and C-CNTs formed with D_{CNT} = ~50 ± 10 nm], (e and f) D_p = ~300 nm, T_G = 500 °C [SU-CNTs formed with D_{CNT} = ~60 ± 13 nm], and (g and h) D_p = ~300 nm, T_G = 700 °C [SU-CNTs formed with D_{CNT} = ~10 ± 4 nm].

particles homogeneously. Since the melting temperature of bulk Al is approximately 660 °C [21], Al components in the seeded Ni particles can be remained if the growth temperature (T_G) of CNTs in the thermal CVD reactor is kept at lower than 660 °C. Therefore, the growth temperature of CNTs was varied to identify the effect of growth temperature on the morphological change of the resulting aerosol CNTs. The growth temperature ranged from 500 °C to 800 °C for the size-selected bimetallic nanoparticles smaller than ~100 nm in diameter.

On the basis of scanning electron microscope (SEM) and transmission electron microscope (TEM) images as shown in Fig. 4a and b, the number concentration of C-CNTs was very high with rarely forming S-CNTs at the medium temperature ranges of 500–650 °C. However, the number concentration of C-CNTs abruptly decreased, and simultaneously, the number concentration of S-CNTs increased at the temperature ranges of 650–800 °C as shown in Fig. 4c and d. This indicates that the solid Al matrix transformed into a liquid-like state at reacting temperatures of higher than ~650 °C (i.e., above the melting point of Al). The liquid-like Al matrix was slowly consumed by CNT precipitation, which finally resulted in leaving Ni sites behind with less Al component in the front side of bimetallic nanoparticles so that S-CNTs are finally tend

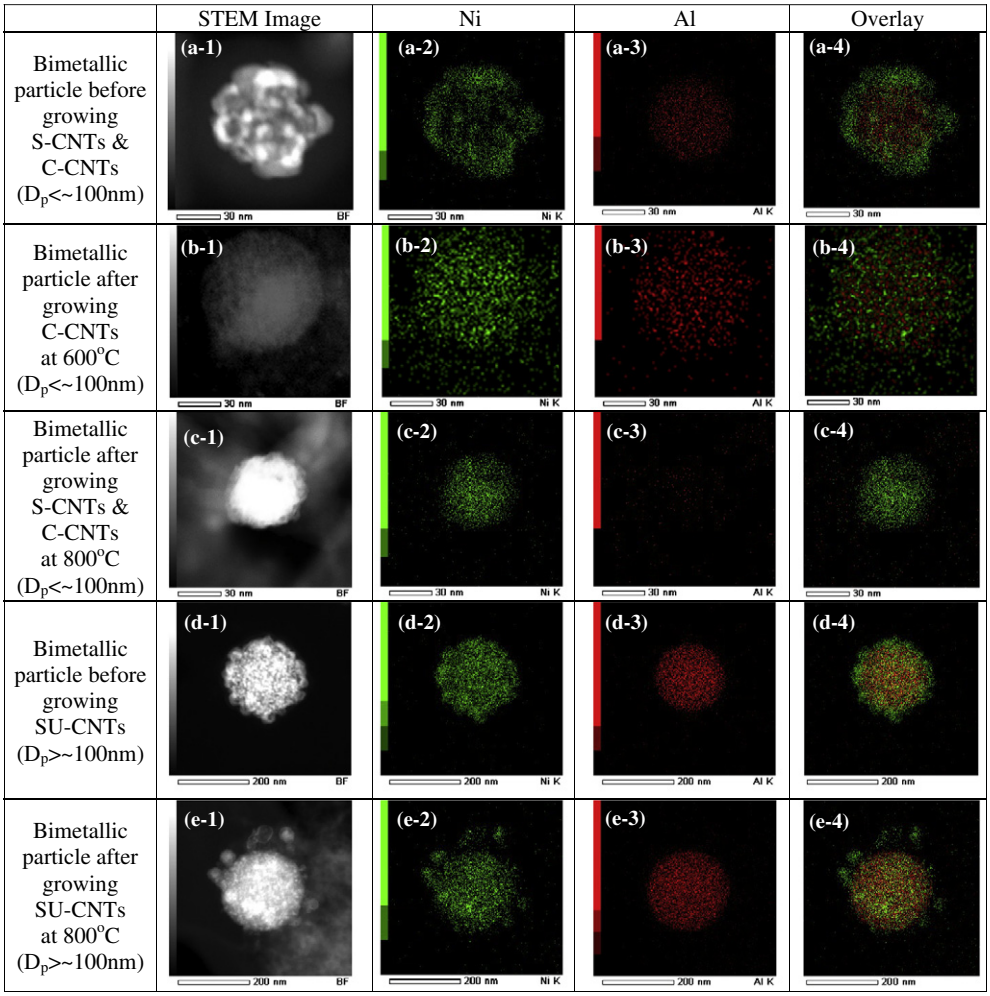

Fig. 5. Elemental mappings of seeded bimetallic particles before and after growing various CNTs at 800 °C in the thermal CVD reactor.

to be grown. This result was corroborated by characterizing the elemental mapping of seeded bimetallic nanoparticles with smaller than ~100 nm before and after growing the mixture of S-CNTs and C-CNTs as shown in Fig. 5a–c. Before growing CNTs as shown in Fig. 5a, both Ni and Al components were homogeneously distributed in the bimetallic nanoparticles. Even after growing the C-CNTs at ~600 °C (Fig. 5b), Al components were still remained in the seeded bimetallic nanoparticles. However, after growing the mixture of S-CNTs and C-CNTs at ~800 °C as shown in Fig. 5c, Al components in the seeded bimetallic nanoparticles were significantly lost, presumably because the molten liquid-like Al components were consumed by the precipitation of CNTs.

Then, we turn our attention to see the effect of reacting temperature on the morphology of SU-CNTs. Spray pyrolized bimetallic nanoparticles with the average size of ~300 nm were fed into thermal CVD reactor to grow aerosol CNTs by mixing with acetylene and hydrogen at 500 °C and 700 °C, respectively.

Interestingly, it is observed as shown in Fig. 4e–h that the diameters of SU-CNTs (D_{CNT}) grown were ~60 ± 13 (Fig. 4e and f) and ~10 ± 4 nm (Fig. 4g and h) at 500 and 700 °C, respectively. It is because the exposed size of Ni sites on the surface of bimetallic nanoparticles seemed to be decreased presumably due to the thermal expansion of Al melted at ~700 °C.

With the assistance of bulk property-based rough estimation, it is noted that the density of liquid-like Al (i.e., 2.4 g/cm^3) melted is smaller than that of solid Al (i.e., ~2.7 g/cm^3), which may result in the thermal expansion of liquid-like Al by ~12% in volume compared with solid Al [22]. In order to produce the SU-CNTs, the average size of bimetallic nanoparticles should be sufficiently large (i.e., D_p > ~100 nm) in this approach so that the multiple Ni sites, which are perfectly isolated by the interference of relatively large Al host matrix sites in the bimetallic nanoparticles, are independently activated and seeded to radially grow CNTs.

Unlike the growth of single CNT (i.e., S-CNT or C-CNT) on the bimetallic nanoparticles with smaller than ~100 nm in diameter, multiple CNTs (i.e., SU-CNTs) were grown on the bimetallic particles with larger than ~100 nm in diameter under broad temperature ranges of 500–800 °C, indicating that isolation of Ni sites seeded was not perturbed by molten state of Al matrix site even at the above of melting temperature of Al, and also Al component was barely consumed by CNT precipitation. It was confirmed by elemental mapping that Al component was homogeneously distributed with Ni component before and after growing SU-CNTs at ~800 °C as shown in Fig. 5c and d.

The possible growth mechanisms of aerosol CNTs with straight, coiled, and sea urchin-like nanostructures are represented in a simplified schematic in Fig. 6. C-CNT is formed on the entire surface of a seeded bimetallic nanoparticle with the average size smaller than ~100 nm at medium temperature ranges of 500–650 °C. However, the number concentration of C-CNTs decreases significantly at relatively high temperature range of 650–800 °C, while S-CNTs can be easily obtained within this temperature range but hardly grown at medium temperature range of 500–650 °C. The growth of S-CNTs results from melting of the Al matrix sites in

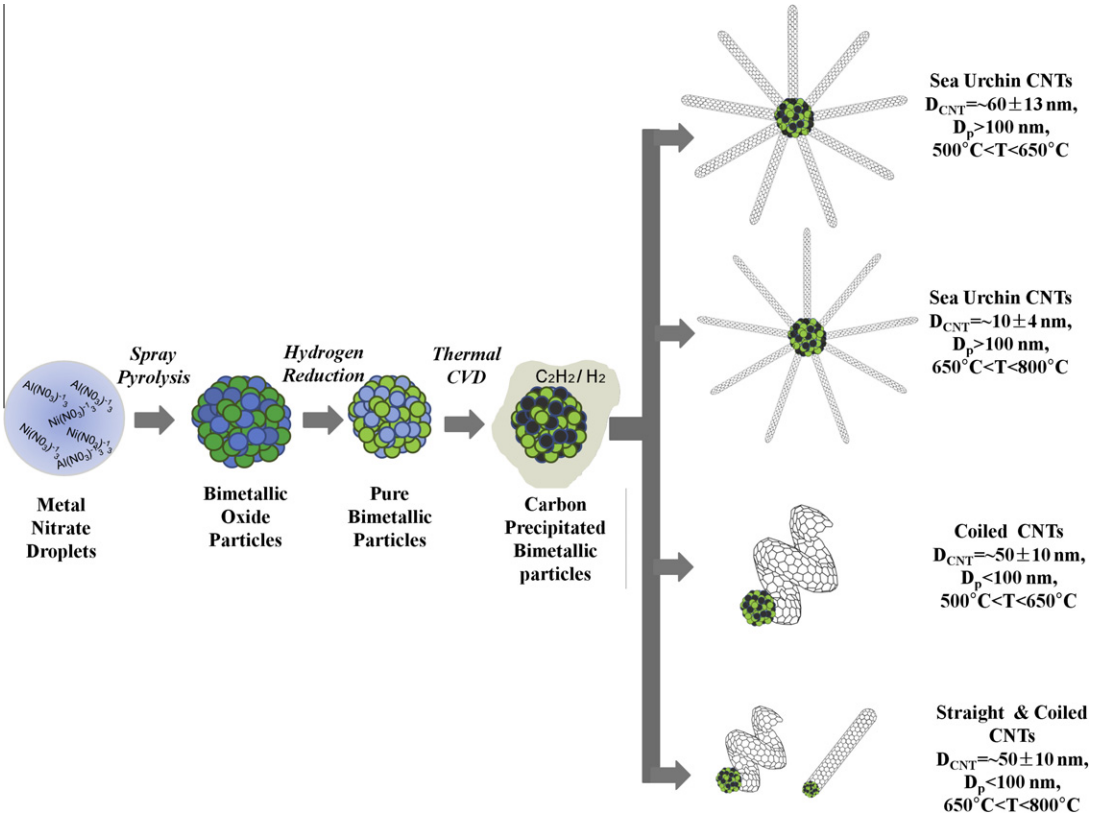

Fig. 6. Schematic of possible growth mechanisms of S-CNTs, C-CNTs, and SU-CNTs on bimetallic composite nanoparticles in the gas phase.

the seeded bimetallic nanoparticles at high temperature range of 650–800 °C so that the liquid-like Al matrix sites are then consumed by subsequent CNT precipitation. Therefore, the presence of Al components in the seeded bimetallic particles with the average size smaller than ~100 nm is the most important in developing the desired morphology for C-CNTs and S-CNTs. However, SU-CNTs are mostly grown on the seeded bimetallic particles with average size larger than ~100 nm, in which Ni sites sufficiently isolated by Al sites are seeded to radially grow multiple CNTs with the average diameter of ~60 ± 13 nm under the medium reaction temperature ranges of 500–650 °C. If the processing takes place at relatively high temperature ranges of 650–800 °C, this makes Al molten and results in significant size reduction of available Ni sites by thermal expansion of non-catalytic Al matrix sites so that one can obtain SU-CNTs with the average diameter of ~10 ± 4 nm.

4. Conclusions

We have demonstrated that we could tailor the morphology of aerosol CNTs with straight, coiled, and sea urchin-like nanostructures in the gas phase by taking advantage of synergistic effect between the size of spray-pyrolized bimetallic nanoparticles (i.e., catalytic Ni sites isolated by non-catalytic Al sites) and the reacting temperature for growing aerosol CNTs in the thermal CVD.

Acknowledgments

This study was supported by the Korea Research Foundation Grant funded by Korean government (MOEHRD) (KRF-2007-313-D00373). This study was also partially supported by the Converging Research Center Program through the National Research Foundation of Korea (NRF) funded by the Ministry of Education, Science and Technology (2009-0081928). The authors also gratefully acknowledge the facility support and technical assistance by Drs. Jin Wook Yoon, Jung Seok Choi, and Yong Taek Kwon from HCT, Inc. for real-time measuring the size distributions of nanoparticles.

References

[1] A. Galano, Chem. Phys. 327 (2006) 159.
[2] R. Saito, G. Dresselhaus, M.S. Dresselhaus, Physical Properties of Carbon Nanotubes, Imperial College Press, London, 1998.
[3] S. Motojima, Y. Noda, S. Hoshiya, Y.J. Hishikawa, J. Appl. Phys. 94 (2003) 2325.
[4] X. Chen, S. Zhang, D.A. Dikin, W. Ding, R.S. Ruoff, L. Pan, Nano Lett. 3 (2003) 1299.
[5] S. Yang, X. Chen, S. Motojima, Carbon 44 (2006) 3352.
[6] S.H. Kim, M.R. Zachariah, Mater. Lett. 61 (2007) 2079.
[7] J.B. Bai, Mater. Lett. 57 (2003) 2629.
[8] J. Liu, A.T. Harris, J. Nanopart. Res. 12 (2009) 645.
[9] M. Monthioux, L. Noe, L. Dussault, J.C. Dupin, N. Latorre, T. Ubieto, E. Romeo, C. Royo, A. Monzon, C. Guimon, J. Mater. Chem. 17 (2007) 4611.
[10] A.G. Nasibulin, A. Moisala, H. Jiang, E.I. Kauppinen, J. Nanopart. Res. 8 (2006) 465.
[11] W.H. Chiang, R.M. Sankaran, Adv. Mater. 20 (2008) 4857.
[12] W.H. Chiang, R.M. Sankaran, Nat. Mater. 8 (2009) 882.
[13] S.H. Kim, M.R. Zachariah, J. Phys. Chem. B 110 (2006) 4555.
[14] A. Moisala, A.G. Nasibulin, S.D. Shandakov, H. Jiang, E.I. Kauppinen, Carbon 43 (2005) 2066.
[15] S.H. Kim, C. Wang, M.K. Zachariah, J. Nanopart. Res. 13 (2011) 139.
[16] E.O. Knutson, K.T. Whitby, J. Aerosol Sci. 6 (1975) 443.
[17] S.H. Kim, K.S. Woo, B.Y.H. Liu, M.R. Zachariah, J. Colloid Interface Sci. 282 (2005) 46.
[18] W. Wang, K. Yang, J. Gaillard, P.R. Bandaru, A.M. Rao, Adv. Mater. 20 (2008) 179.
[19] N.K. Chang, S.H. Chang, Carbon 46 (2008) 1106.
[20] S. Amelinckx, X.B. Zhang, D. Bernaerts, X.F. Zhang, V. Ivanov, J.B. Nagy, Science 265 (1994) 635.
[21] Y.F. Zhu, J.S. Lian, Q.J. Jiang, J. Phys. Chem. C 113 (2009) 16896.
[22] A. Rai, D.G. Lee, K.H. Park, M.R. Zachariah, J. Phys. Chem. B 108 (2004) 14793.